# Evaluation of terahertz density of vibrational states from specific-heat data: Application to silica glass

N. V. Surovtsev
*Institute of Automation and Electrometry, Russian Academy of Sciences, pr. Ak. Koptyuga 1, Novosibirsk, 630090, Russia*
(Received 18 June 2001; published 14 November 2001)

The efficiency of the Tikhonov regulation method for the specific-heat phonon spectrum inversion problem is demonstrated. The regulation method is applied to the evaluation of the density of vibrational states from the low-temperature specific heat of a silica glass. The density of states obtained is found to be in good agreement with the results of inelastic neutron scattering. The extracted density of states is used for the analysis of the Raman light-vibration coupling coefficient. It is established that the coupling coefficient increases with frequency faster than $\propto \nu$ at $\nu < 10\ \mathrm{cm}^{-1}$. In the frequency range above $10\ \mathrm{cm}^{-1}$ the coupling coefficient is found to be in agreement with the results of previous investigations.

DOI: 10.1103/PhysRevE.64.061102 PACS number(s): 63.50.+x, 64.70.Pf, 63.20.Pw

## I. INTRODUCTION

The density of vibrational states is an important characteristic in the physics of condensed matter [1]. In recent years the efforts of many research groups have gone into the study of terahertz vibrational excitations in glasses [2]. It is known that the density of vibrational states $g(\nu)$ in glasses shows a deviation from the Debye approximation [$g(\nu) \propto \nu^2$] in the terahertz frequency range, leading to the appearance of a peak in $g(\nu)/\nu^2$ presentation (the so-called boson peak). Since the terahertz dynamics of glass formers is considered to be very important for understanding glass properties and the phenomenon of the glass transition, various experimental techniques have been used to study the terahertz vibrational states: low-temperature specific heat and thermal conductivity [2], inelastic neutron scattering [3] and x-ray scattering [4], infrared absorption [5], and low-frequency Raman scattering [6]. In spite of the variety of these experimental techniques only inelastic neutron scattering is able to measure the density of vibrational states without an additional frequency dependent function.

Although inelastic neutron scattering plays a great role in measuring the vibrational density of states, this experimental technique is too expensive and not sufficiently accessible to be a routine experimental technique for most researchers dealing with a variety of different glassy materials. Thus an alternative experimental technique is very desirable. One possibility could be related to the analysis of low-temperature specific-heat data.

Indeed, the specific heat $C_V(T)$ is an integral over the density of states. An expression for the low-temperature specific heat per unit mass is obtained by differentiation of the vibrational energy with respect to temperature [1],

$$C_V(T) = k_B \int_0^\infty g(\nu)(h\nu/k_BT)^2 \frac{\exp(h\nu/k_BT)}{[\exp(h\nu/k_BT)-1]^2} d\nu. \tag{1}$$

Here $k_B$ is Boltzmann's constant. Since the difference between $C_V(T)$ and $C_P(T)$ can be neglected for condensed substances, the experimentally measured $C_P(T)$ can be taken as a good approximation for Eq. (1).

The inversion problem for Eq. (1) is quite old and several approaches have been used for solving it (for example, [7–9]). Very recently [9], it was shown that an approach based on the Mobius inversion formula is appropriate for the problem and a good qualitative solution was obtained. However, to our knowledge no simple procedures allowing the evaluation of $g(\nu)$ from experimental specific-heat data are giving good qualitative agreement with the density of states from neutron scattering results have been proposed. In previous work devoted to this problem the exact inversion operator was constructed. But for practical use it is important that the inversion problem of an integral equation like Eq. (1) is an ill-posed problem from the mathematical point of view [10]. The solution of the integral equation is highly unstable for small perturbations in the left side of Eq. (1). This instability is the reason for the complexity of the problem. Recently, in [11] it was shown that the Tikhonov regulation method [10] can be successfully applied for solving Eq. (1). Thus the open question is whether this method can extract $g(\nu)$ of a glass in good quantitative agreement with neutron data.

The goal of the present work is twofold: the first is the check whether the terahertz density of states of a glass found by the regulation method is in agreement with neutron scattering data with good precision; the second goal is to demonstrate an application of the evaluated density of states to a problem where the use of low-temperature $g(\nu)$ is important. It will be shown that the evaluated $g(\nu)$ of a silica glass is in excellent quantitative agreement with the results of neutron scattering experiments. The evaluated $g(\nu)$ corresponding to the density of states at very low temperatures ($\sim 10$ K) is applied to the problem of the Raman coupling coefficient, where the low-temperature $g(\nu)$ is essential in order to avoid the fast relaxation contribution. The results are compared with the coupling coefficient found in previous work of Sokolov *et al.* [12] and Fontana *et al.* [13].

## II. METHOD

Since the low-temperature specific heat increases strongly as temperature increases, it is more convenient to rewrite Eq.

 

(1) in such a way that the left side of the equation has no sharp increases. This goal can be achieved by division of Eq. (1) by $T^3$. Thus, the problem considered is the inversion of the equation

$$\frac{C_V(T)}{T^3}=\int_0^\infty g'(\nu)F(\nu,T)d\nu \tag{2}$$

where

$$g'(\nu)=g(\nu)k_B,$$

$$F(\nu,T)=\frac{(h\nu/k_BT)}{T^3}\frac{\exp(h\nu/k_BT)}{[\exp(h\nu/k_BT)-1]^2}.$$

Considering Eq. (2) at $N$ discrete values of temperature, limiting the frequency integration by $\nu_{\max}$, and changing the integral in Eq. (2) to a sum with $M$ equidistant steps $\Delta\nu=\nu_{\max}/M$, one obtains the system of linear equations

$$\sum_{j=1}^{M} A_{ij}x_j=y_i, \qquad i=1,\ldots,N \tag{3}$$

where

$$y_i=C_V(T_i)/T^3,$$

$$A_{ij}=\frac{F((j-1)\Delta\nu,T_i)+F(j\Delta\nu,T_i)}{2}\Delta\nu,$$

$$x_j=\frac{g'((j-1)\Delta\nu)+g'(j\Delta\nu)}{2}.$$

The solution of the system (3) can be found by minimization of the functional

$$\Phi_\alpha=\Phi_o+\alpha\Phi_r \tag{4}$$

where

$$\Phi_o=\sum_{i=1}^{N}\left(\sum_{j=1}^{M}A_{ij}x_j-y_i\right)^2, \tag{5}$$

$$\Phi_r=\sum_{j=2}^{M}\frac{(x_j-x_{j-1})^2}{\Delta\nu}. \tag{6}$$

The functional $\Phi_o$ [Eq. (5)] reflects the demand for the best solution for the system (3) and the functional $\Phi_r$ minimizes the first derivative of the solution. The functional $\Phi_r$ is added because for physical reasons the true solution of Eq. (1) must be a smooth function. $\Phi_r$ allows one to avoid discontinuous or quickly oscillating solutions. $\alpha$ is the so-called regulation parameter [10], which controls the relative weight of the stabilizing functional $\Phi_r$ in the total functional $\Phi_\alpha$. The minimum of $\Phi_\alpha$ is achieved when all particular derivatives are equal to zero:

$$\frac{\partial\Phi_\alpha}{\partial x_j}=0.$$

This requirement leads from Eq. (3) to

$$\sum_{i=1}^{N}\sum_{k=1}^{M}A_{ik}A_{ij}x_k+\sum_{k=1}^{M}\frac{\alpha}{\Delta\nu}D_{jk}x_k=\sum_{i=1}^{N}A_{ij}y_i \tag{7}$$

where

$$D_{jk}=\begin{pmatrix} 1 & 0 & 0 & 0 & 0 & \ldots & 0\\ -1 & 2 & -1 & 0 & 0 & \ldots & 0\\ 0 & -1 & 2 & -1 & 0 & \ldots & 0\\ 0 & 0 & -1 & 2 & 1 & \ldots & 0\\ \ldots & \ldots & \ldots & \ldots & \ldots & \ldots & \ldots\\ 0 & 0 & 0 & 0 & 0 & \ldots & 1 \end{pmatrix}.$$

In general, the solution of Eq. (7) depends on the magnitude of the parameter $\alpha$. When $\alpha$ is too low, discontinuous or oscillating components appear in the solution. When $\alpha$ is high, the solution becomes too smooth, deviating significantly from the true solution of the problem. To strike a compromise for the magnitude of $\alpha$, in [11] it was proposed to control the parameter $\gamma$, where

$$\gamma=\int\left[\frac{\partial}{\partial\nu}\left(\frac{g(\nu)}{\nu^2}\right)\right]^2 d\nu. \tag{8}$$

This parameter increases sharply when in any density of states $g(\nu)$ oscillating components appeared. Thus, by analyzing the behavior of $\gamma$ versus $\alpha$, it is possible to choose an optimal regulation parameter, when the oscillating components are still suppressed but the mean square deviation $\chi_S$ is minimal:

$$\chi_S=\sqrt{\frac{1}{N}\sum_{T_{\min}}^{T_{\max}}\left(\frac{C_V(T)-C_V^*(T)}{C_V(T)}\right)^2}. \tag{9}$$

Here $T_{\min}$ and $T_{\max}$ depict the temperature interval and $C_V^*(T)$ is the calculated specific heat for the found $g(\nu)$. The validity of the parameter $\gamma$ for revealing the oscillating components was illustrated in [11].

The limited temperature range where $C_V(T)$ is measured leads to a limited frequency range $\nu_{\min}-\nu_{\max}$ where a reliable $g(\nu)$ can be found. Since the curve $C_V(T)/T^3$ for a vibration with frequency $\nu$ has a sharp maximum at a temperature $\approx 0.2h\nu/k_B$, a rough estimate leads to

$$\nu_{\min}=5k_BT_{\min}/h,$$

$$\nu_{\max}=5k_BT_{\max}/h. \tag{10}$$

Testing for the Debye density of states in [11] shows that the estimation (10) is approximately obeyed. Also, in [11] the empirical result was obtained that the considered frequency range should not be smaller than $\sim 2.5\nu_{\max}$ in order to avoid

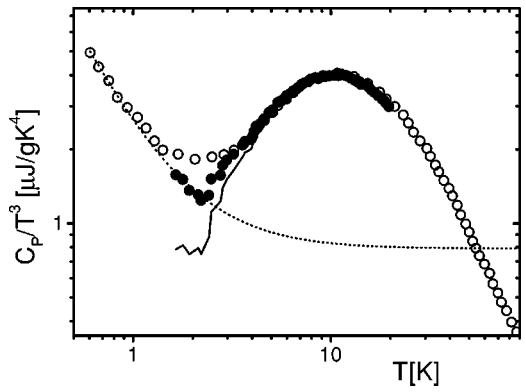


FIG. 1. Specific heat of $SiO_2$ glass in $C_P(T)/T^3$ presentation. Open circles are data of Ref. [15], solid circles of Ref. [14]. Dotted line is the low-temperature approximation from the Debye limit plus TLS contribution. Solid line is the data of Ref. [14] with TLS contribution subtracted.

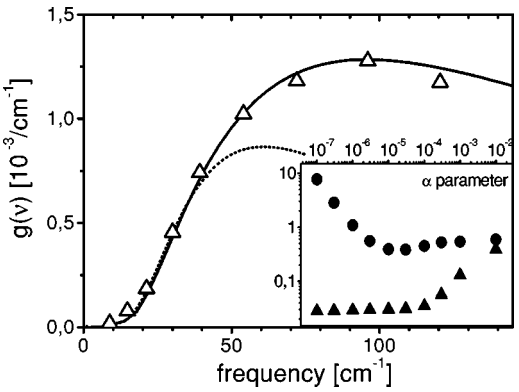


FIG. 2. Density of vibrational states evaluated from the specific heat. Solid line corresponds to data of [15] and dotted line to data of [14]. Triangles are density of states found by inelastic neutron scattering [14]. Inset shows the average mean square deviation (triangles) and parameter $\gamma$ (circles) versus regulation parameter $\alpha$.

distortion of the evaluated density of states due to a contribution from vibrational excitations with frequencies higher than $\nu_{\max}$.

If there is information *a priori* about the frequency behavior of $g(\nu)$, then the parameter $\alpha$ can be taken as frequency dependent. For example, if the behavior of $g(\nu)$ is expected to increase not more slowly than $\propto \nu^2$, it is natural to take the regulation parameter proportional to the inverse of the square of the derivative of $g(\nu)$:

$$\alpha \propto \frac{1}{\nu^2}. \tag{11}$$

This kind of regulation takes into account the tendency of the derivative of $g(\nu)$ to increase linearly or faster as the frequency increases and controls relative contribution of the functional $\Phi_r$ in Eq. (4) according to this tendency. As it will be demonstrated below, expression (11) improves the quality of the low-frequency part of $g(\nu)$, for which the temperature range below the maximum of $C_P(T)/T^3$ dominates in the evaluation. Note that the expression (11) should not be used for the whole frequency range, since it reduces the quality of the evaluation for the high-frequency part of the spectrum.

### III. RESULTS

The method described was realized in a computer program using the Gauss method for solving the system (7). The low-temperature specific-heat data of $SiO_2$ glass used in the evaluation are presented in Fig. 1. Two sources of specific-heat data were used. The data for a Heralux silica glass measured in Ref. [14] have a rather limited temperature range, but the advantage of these data is that $g(\nu)$ is known from inelastic neutron scattering for the same glass. Also, the specific-heat data from [15] with a much broader temperature range were used in the evaluation. Since the data of Ref. [15] coincide well with the data of [14] (Fig. 1), results for them will also be compared with the density of states found in Ref. [14].

The specific heat below 1 K in glasses is dominated by the contribution from two-level systems (TLS's). In order to remove the TLS contribution from the experimental data the low-temperature Debye limit plus a TLS contribution in the functional form $\propto T^{-1.65}$ were used for the description of the specific heat below 2 K (Fig. 1; the value $-1.65$ of the exponent was chosen by a fit of the low-temperature limit of the experimental curve). Then the TLS contribution found in this way was subtracted from the specific-heat data.

The inset of Fig. 2 illustrates the procedure for the choice of the parameter $\alpha$ described in the previous section. It is seen that the mean square deviation $\chi_S$ decreases quickly with decreasing $\alpha$ for $\alpha > 3\times10^{-5}$ and is almost constant at $\alpha < 3\times10^{-5}$ [this constant limit arises from the statistical scatter of experimental points of $C_V(T)$]. On the other hand, the parameter $\gamma$ strongly increases for $\alpha < 3\times10^{-5}$, indicating the appearance of an oscillating artifact in the calculated density of states. Thus, from the inset of Fig. 2 it is clear that the optimal value of $\alpha$ is about $3\times10^{-5}$. The evaluated density of states at the optimal parameter $\alpha = 3\times10^{-5}$ recovers the experimental specific heat with average precision $\approx 3\%$.

The dotted line in Fig. 2 shows the density of states evaluated from the specific-heat data of Ref. [14]. The density of states taken from neutron scattering experiments is also shown in this figure. It is seen that the calculated $g(\nu)$ is reliable up to 40 cm$^{-1}$ [the estimation from Eq. (10) gives $\nu_{\max} \sim 70$ cm$^{-1}$]. The density of states evaluated from data of Ref. [15] is shown by the solid line. Note the excellent agreement between the neutron scattering data and the evaluated density of states over the whole frequency range up to 120 cm$^{-1}$. The agreement between the absolute values of the evaluated $g(\nu)$ and those from neutron scattering is noticeable.

Figure 3 presents the density of states in the low-frequency part of the spectrum. The solid line in this figure corresponds to the evaluated density of states, where for the low-frequency part of spectrum the regularization method with $\alpha \propto \nu^{-2}$ was applied. The figure proves that the regulation parameter in the form of expression (11) allows a reduction of the scatter in the low-frequency part of $g(\nu)$, giving results in good accordance with the average behavior of the

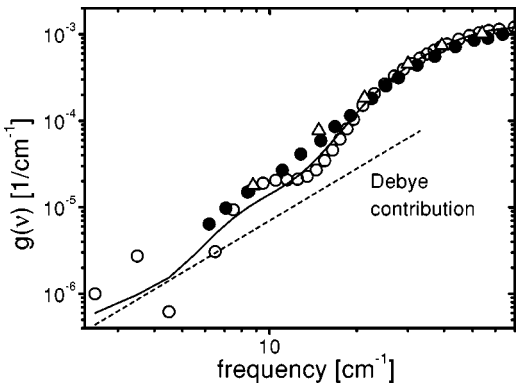


FIG. 3. Low-frequency part of density of vibrational states. Open circles are $g(\nu)$ calculated from [15] with $\alpha=$const; solid line is $g(\nu)$ calculated with $\alpha \propto \nu^{-2}$. Results of neutron scattering at room temperature shown by triangles and at 51 K by closed circles (data from [14] and [13], respectively). Dashed line is Debye behavior calculated from density and sound velocity.

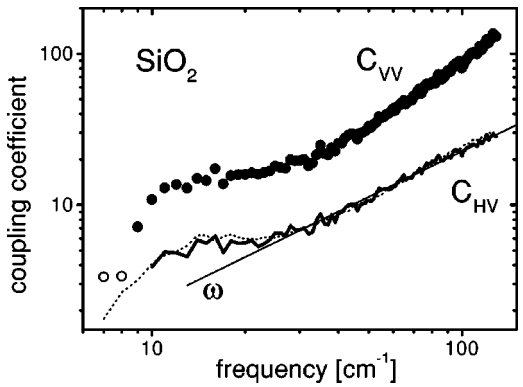


FIG. 4. Light-vibration coupling coefficient $C(\nu)$. Circles are for polarized Raman scattering (Raman data from Ref. [18]) (open symbols explained in the text); thick line is for depolarized Raman scattering. Dotted line is the coupling coefficient for depolarized Raman data of Ref. [19]. Thin line is $\propto \nu$ behavior.

result for $\alpha=$const. The general behavior of the evaluated density of states is in good agreement with the results of neutron scattering at room temperature and at $T=51$ K. However, in the frequency range $\nu<20$ cm$^{-1}$ the evaluated $g(\nu)$ is lower than that from neutron scattering. This difference might be explained by a contribution of the fast relaxation to the neutron spectra. Indeed, from Raman scattering experiments it is known that the fast relaxation contributes significantly to the spectra at $T\approx 50$ K, while the contribution becomes very low at $T<10$ K in the frequency range considered [16,12]. The effective temperature for the evaluated density of states is lower than in the neutron experiments, being about 10 K or less. Thus, the contribution of the fast relaxation is more highly suppressed for $g(\nu)$ found from the low-temperature specific-heat data in comparison with the neutron data. In the frequency range below 7 cm$^{-1}$ the evaluated $g(\nu)$ comes close to the Debye density of states calculated from the macroscopic values for silica glass (Fig. 3).

It was also checked whether the precision of the subtraction procedure of the TLS contribution influences the precision of the $g(\nu)$ found. For this goal the $g(\nu)$ found was compared with the solution evaluated from the specific heat without subtraction of the TLS contribution. In the frequency range considered ($>2$ cm$^{-1}$) only minor changes were found in the densities of states $g(\nu)$ evaluated from the specific heat with and without the TLS contribution. This is easily explained since the TLS contribution quickly decreases with increasing $T$, which virtually corresponds to additional vibrations below the discussed frequency range. Therefore, in the considered spectral range the results obtained do not depend on the way the TLS contribution was subtracted.

## IV. DISCUSSION

The results presented in the previous section show good agreement between the densities of vibrational states evaluated from the low-temperature specific heat and found in inelastic neutron scattering. Thus, the good efficiency of the regulation method for the specific-heat phonon spectrum inversion problem is demonstrated. Moreover, the evaluated density of states corresponds to lower temperatures than usually measured in neutron scattering experiments, and, therefore, has a much smaller or negligible contribution from the fast relaxation. The last fact shows the good applicability of the evaluated density of states for topics where the suppression of the fast relaxation is essential.

One such topic is the analysis of the so-called light-vibration coupling coefficient $C(\nu)$, which relates Raman scattering spectra with the density of states via the Shuker-Gammon relation [17]

$$I(\nu)=C(\nu)g(\nu)\frac{[n(\nu,T)+1]}{\nu},$$

where $I$ is the intensity of the Stokes side of the Raman spectrum and $n$ is the Bose factor. In [12] it was shown that the coupling coefficient is proportional to frequency in the spectral range 10–120 cm$^{-1}$. However, in the recent work [13], where significant attention was paid to the low-frequency limit of the coupling coefficient, it was demonstrated that $C(\nu)$ has a linear behavior in the frequency range 10–90 cm$^{-1}$ with a nonvanishing value in the $\nu\rightarrow 0$ limit. In that work the effective temperature for the coupling coefficient was 51 K. In the present work we reexamine this result using the evaluated density of states. Before discussion, we should note that in [13] the authors used different kinds of silica glass for light scattering (Suprasil) and for the neutron experiments (Heralux). Such discordance should lead to a distortion of results since the low-frequency spectra of Heralux and Suprasil are slightly different.

For evaluation of the coupling coefficient the right-angle Raman data at $T=7$ K of Heralux glass published in [18] were used. The coupling coefficients found for polarized and depolarized Raman scattering are shown in Fig. 4, where the evaluated density of states from Fig. 3 was used. Also, in Fig. 4 the coupling coefficient calculated for the depolarized Raman data at $T=10$ K from [19] is added for comparison.

The good agreement between the different curves demonstrates the validity of the low-temperature Raman data. The line with $\propto \nu$ behavior in Fig. 4 allows one to stress, that while the behavior in the range 30–100 $cm^{-1}$ follows the frequency proportionality well, in the lower-frequency range there is a significant flatness of the curve. Thus, our result confirms the observation of Ref. [13] that in the range 10–30 $cm^{-1}$ the coupling coefficient does not follow $\propto \nu$ behavior.

Moreover, Fig. 4 demonstrates that below 10 $cm^{-1}$ $C(\nu)$ has different behavior from above 10 $cm^{-1}$. The lowest points of $C(\nu)$ increase with increasing frequency even faster than $\propto \nu$. In the Raman experiment of Ref. [18] the signal in the range 7–8 $cm^{-1}$ was so weak that it was not possible to detect it. In this case only an estimation of the upper limit of the signal can be made. This estimate was used for the calculation of the upper limit of $C(\nu)$ at frequencies 7–8 $cm^{-1}$. In Fig. 4 the open circles show the upper limit of the coupling coefficient (for the polarized spectrum). Thus, it is very likely that the behavior of $C(\nu)$ observed in [13] is restricted to the range only down to 10 $cm^{-1}$, but at $\nu<10$ $cm^{-1}$ the coupling coefficient has another frequency dependence. Also, from the data of [19] it follows that $C(\nu)$ increases faster than $\propto \nu$ at $\nu<10$ $cm^{-1}$, but not so fast as calculated from the data of [18]. Further measurements of Raman scattering in silica glass at low frequencies ($<10$ $cm^{-1}$) and low temperatures ($<10$ K) are needed in order to clarify the functional behavior of the coupling coefficient at $\nu<10$ $cm^{-1}$. However, Fig. 4 demonstrates that at least it is faster than $\propto \nu$.

Figure 5 compares the coupling coefficient obtained in the present work with those from previous work [12] and [13] at corresponding temperatures near 50 K. A good agreement in the frequency range 10–60 $cm^{-1}$ is seen for different data. Above this frequency there is a deviation from the $\propto \nu$ behavior for the data of Ref. [13]. The flatness of the data from Ref. [13] at above 60 $cm^{-1}$ is at least partly related to the different kinds of silica glass used in the Raman and neutron experiments. The data of the present work continue the $\propto \nu$ behavior with good precision at least up to 130 $cm^{-1}$.

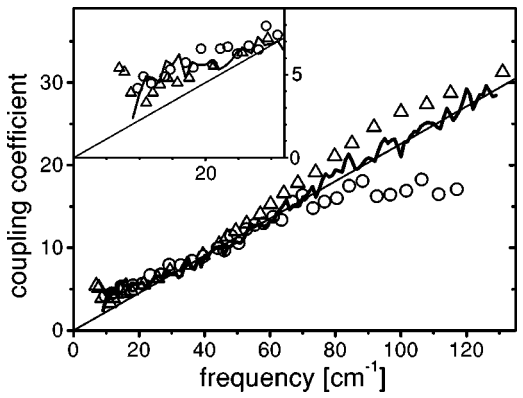


FIG. 5. Light-vibration coupling coefficient $C(\nu)$ for depolarized Raman scattering. Thick line is the result of present work. Triangles are data from [12]. Circles are data from [13]. Straight line is $\propto \nu$ behavior. Inset shows the low-frequency part of $C(\nu)$ in detail.

## V. CONCLUSION

In the work the density of vibrational states $g(\nu)$ is evaluated by the Tikhonov regulation method from the experimental low-temperature specific heat of a silica glass. Good quantitative agreement between the evaluated density of states and the results of inelastic neutron scattering is obtained. Thus, the efficiency and reliability of the method applied for the extraction of the density of states from specific-heat data without any model suppositions are demonstrated. This relatively simple method of evaluation of $g(\nu)$ opens possibilities for researchers in the physics of glasses. The evaluated density of states corresponds to an effective temperature $\sim 10$ K. It was shown that the density of states obtained could be used for an analysis of the Raman light-vibration coupling coefficient at low temperatures. The present analysis reproduces the results for silica glasses obtained in previous work [12,13] in the range $\nu>10$ $cm^{-1}$ and gives an indication that at frequencies below 10 $cm^{-1}$ the coupling coefficient increases with increasing frequency faster than $\propto \nu$.

## ACKNOWLEDGMENTS

This work was supported by the Interdisciplinary Science Fund at the Russian Foundation for Basic Research of the Siberian Division of the Russian Academy of Sciences (Project 7) and by RFFI Grants No. 99-02-16697 and No. 01-05-65066.

[1] C. Kittel, *Introduction to Solid State Physics* (John Wiley and Sons, New York, 1986).
[2] *Amorphous Solids: Low-Temperature Properties*, edited by W. A. Phillips (Springer, Berlin, 1981).
[3] U. Buchenau, N. Nucker, and A.J. Dianoux, Phys. Rev. Lett. **53**, 2316 (1984).
[4] P. Benassi, M. Krisch, C. Masciovecchio, V. Mazzacurati, G. Monaco, G. Ruocco, F. Sette, and R. Verbeni, Phys. Rev. Lett. **77**, 3835 (1996).
[5] U. Storm and P.C. Taylor, Phys. Rev. B **16**, 5512 (1977).
[6] J. Jackle, in *Amorphous Solids: Low-Temperature Properties* Ref. [2].
[7] I.M. Lifshitz, Zh. Eksp. Teor. Fiz. **26**, 551 (1954).
[8] N.X. Chen, Phys. Rev. Lett. **64**, 1193 (1990).
[9] D.M. Ming, T. Wen, J.X. Dai, X. Dai, and W.E. Evenson, Phys. Rev. E **62**, R3019 (2000); D.X. Xi, T. Wen, G.C. Ma, and J.X. Dai, Phys. Lett. A **264**, 68 (1999).
[10] A. N. Tikhonov and V. Ya. Arsenin, *Methods of Solutions of Ill-Posed Problems* (Nauka, Moscow, 1974) (in Russian).
[11] N. V. Surovtsev, Avtometriya No. 4, 65 (2001) (in Russian).
[12] A.P. Sokolov, U. Buchenau, W. Steffen, B. Frick, and A. Wischnewski, Phys. Rev. B **52**, R9815 (1995).

[13] A. Fontana, R. Dell'Anna, M. Montagna, F. Rossi, G. Viliani, G. Ruocco, M. Sampoli, U. Buchenau, and A. Wischnewski, Europhys. Lett. **47**, 56 (1999).
[14] U. Buchenau, M. Prager, N. Nucker, A.J. Dianoux, N. Ahmad, and W.A. Phillips, Phys. Rev. B **34**, 5665 (1986).
[15] Y. Inamura, M. Arai, Yamamuro, A. Inaba, N. Kitamura, T. Otomo, T. Matsuo, S.M. Bennington, and A.C. Hannon, Physica B **263-264**, 299 (1999).
[16] G. Winterling, Phys. Rev. B **12**, 2432 (1975).
[17] R. Shuker and R.W. Gammon, Phys. Rev. Lett. **25**, 222 (1970).
[18] N.V. Surovtsev, J. Wiedersich, V.N. Novikov, E. Rössler, and E. Duval, Phys. Rev. Lett. **82**, 4476 (1999).
[19] A.P. Sokolov, V.N. Novikov, and B. Strube, Europhys. Lett. **38**, 49 (1997).